Water Clustering and Percolation in Low Hydration DNA Shells

Ivan Brovchenko,*,† Aliaksei Krukau,† Alla Oleinikova,† and Alexey K. Mazur*,‡

Physical Chemistry, Dortmund University, Otto-Hahn-Str. 6, Dortmund D-44227, Germany, CNRS UPR9080, Institut de Biologie Physico-Chimique, 13, rue Pierre et Marie Curie, Paris 75005, France

Received: December 20, 2006; In Final Form: January 23, 2007

The hydrogen-bonded networks of water at the surface of a model DNA molecule are analyzed. At low hydrations, only small water clusters are attached to the DNA surface, whereas, at high hydrations, it is homogeneously covered by a spanning water network. The spanning water network is formed via a percolation transition at an intermediate hydration number of about 15 water molecules per nucleotide, which is very close to the midpoint of polymorphic transitions between A- and B-forms of the double helix. The percolation transition can occur in both A- and B-DNA hydration shells with nearly identical percolation thresholds. However, the mechanism of the percolation transition in A- and B-DNA is qualitatively different in regard to the roles played by the two opposite grooves of the double helix. Free ions can shift the percolation threshold by preventing some water molecules from hydrogen bond networking. The results corroborate the suggested relationship between water percolation and the low hydration polymorphism in DNA.

1. Introduction

The presence of water at the surface of biomolecules is necessary for their conformational stability and function. The minimal amount of water depends on the biomolecule and the function considered. It was found that a number of proteins rapidly recover biological activity when hydration water forms an infinite hydrogen-bonded (H-bonded) network.[1−7] This water network appears via a quasi-2D percolation transition at a particular hydration level called a percolation threshold. Below the percolation threshold, the hydration water exists as an ensemble of small clusters, whereas, above the threshold, the H-bonded water network spans the whole system. During the recent years, the percolation transition of hydration water was experimentally detected in a variety of biosystems.[8−11] Molecular dynamics (MD) simulations of hydrated protein powders revealed a quasi-2D percolation transition, with an infinite H-bonded network formed at a hydration threshold close to the experimental value.[12]

Dynamics and functions of proteins are often completely restored when they are covered by about a monolayer of hydration water.[7,13] On model finite hydrophilic surfaces, such a monolayer is formed via a quasi-2D percolation transition characterized by a number of distinct features,[14−17] which made possible a quantitative analysis of water clustering and percolation in hydration of biomolecules. Notably, the appearance of the first water monolayer on a protein surface corresponds to the formation of an H-bonded water network that spans the whole surface of a biomolecule. The center of mass of such a *spanning* water network is close to the center of mass of the biomolecule, indicating homogeneous water coverage.[17] In a variety of protein systems, a spanning water network emerges via a quasi-2D percolation transition similarly to model hydrophilic spheres.[12,17−19] This was shown for hydration of a single lysozyme molecule,[12,17] for cooling of SNase and elastin-like peptide in dilute solutions,[18] and for pressurization of a crystalline SNase.[19]

The water percolation transition is arguably related to the conformational dynamics of hydrated biomolecules;[16,18] however, the microscopic origin of this relationship is unclear. It was suggested that the spanning network of hydration water facilitates the protein conformational mobility[7] and the charge transport along its surface.[1] Another factor to be considered is a strong increase of water density fluctuations at the percolation transition that may accelerate conformational transitions. A reasonable approach to this problem consists of studying various properties of hydrated biomolecules when crossing the water percolation threshold.

Hydration of nucleic acids has a number of distinctions due to their polyionic character and uneven nonspherical shapes.[20] Under physiological conditions, the double helical DNA directly interacts with solvent ions at several water layers from its surface; therefore, the functional DNA hydration shell is very thick. Under limited hydration, there is a strict relationship between the state of DNA and the hydration number (Γ) measured as the number of water molecules per nucleotide (or phosphate). When Γ is reduced below 30, the common B-form of DNA is already perturbed, but it is maintained until $\Gamma \approx 20$.[20,21] Below this hydration, DNA undergoes different conformational transitions depending upon its sequence, bound metal ions, and other environmental conditions. The most studied is the transition from the B- to A-form,[22] with the midpoint at about $\Gamma = 15$.[20,23,24] Another low hydration state of DNA compatible with any base pair sequence, C-DNA, is poorly studied and probably structurally dissimilar to both A- and B-DNA.[25] A few other low hydration forms were found for special DNA sequences.[21,26]

The physics and the driving forces of the low hydration polymorphic transitions in DNA are elusive. Recent MD simulations of B ↔ A transitions of DNA in small water droplets attributed the immediate cause of the B-to-A transition to accumulation of free metal ions in the major B-DNA groove.[27,28] The important role of the condensed ions is evident because

* To whom correspondence should be addressed. E-mail: brov@heineken.chemie.uni-dortmund.de (I.B.); alexey@ibpc.fr (A.K.M.).

† Dortmund University.

‡ CNRS UPR9080.

10.1021/jp068776v CCC: $37.00
Published on Web 03/08/2007

they cannot leave DNA upon dehydration and their mole fraction becomes high under low hydration. There are strong reasons to believe, however, that behind this visible process some hidden drastic changes in water structure develop under $\Gamma < 20$. For instance, B-to-A transitions also occur in concentrated solutions of some nonpolar alcohols.[29] Interestingly, this takes place only in alcohols that can precipitate DNA and the transition occurs very close to the point of precipitation.[30]

In our recent Letter,[31] we reported the first simulation study of the percolation transition of hydration water at the surface of a model B-DNA molecule. It was found that the breakdown of the spanning water network upon dehydration occurs close to the midpoint of the polymorphic transition from the B-form to low hydration forms.[20,23,24] In addition, the long-range mobility of ions in the DNA hydration shell was found to be strongly accelerated in the presence of the spanning water network in good agreement with the experimental DNA conductivity.[32] To shed new light on the possible role of water percolation in DNA polymorphic transitions, here we study the evolution of the key clustering properties of hydration water on the surface of model B- and A-DNA molecules in the presence of Na^+ counterions. It appears that the water percolation transition occurs in both B- and A-DNA hydration shells but in the opposite grooves. In both cases, the percolation threshold is close to the midpoint of the B-to-A transition. Free ions shift the threshold by hampering H-bonded networking for water molecules of their coordination shells. The results further corroborate the suggested relationship between water percolation and the low hydration polymorphism in DNA.

2. Methods

Molecular dynamics (MD) simulations were carried out for hydration shells around a dodecamer fragment of double helical DNA (CGCGAATTCGCG). The structures of the canonical B-DNA and A-DNA[33] were fixed in space. At the present stage of our studies, fixed experimental DNA structures are preferable because, with the currently available force fields, they are likely to approximate real contact surfaces better than flexible DNA. The Cornel et al. force field[34] was used for DNA and the TIP3P model[35] for water. The MD simulations were carried out with the internal coordinate molecular dynamics (ICMD) method adapted for DNA[27,28,36−38] with a time step of 0.01 ps. The system involved 24 bases and 22 phosphate groups in two DNA strands surrounded by a mobile hydration shell of 22 Na^+ ions and 24Γ water molecules, with Γ values varying from 10 to 30. Such water drops were placed in a vacuum with natural infinite boundary conditions. The electrostatic interactions were computed without cutoffs by using the Smooth Particle Mesh Ewald method[39] adapted for infinite boundaries as described elsewhere.[36] The common values of Ewald parameters were used, that is, 9 Å truncation for the real space sum and $\beta \approx 0.35$.

The starting states were prepared as follows. The DNA fragment was first immersed in a large rectangular water box, and the extra water molecules were removed by using a spherical distance cutoff from DNA heavy atoms. The cutoff distances were adjusted to obtain the desired hydration numbers (Γ). The hydrated B- and A-DNA fragments were neutralized by randomly placing 22 Na^+ ions within the hydration shell. When hydration was studied in the absence of ions, the neutralized DNA was obtained either by reducing the charge of phosphate oxygens by $0.5e$ (phosphate neutralization) or by uniformly distributing the neutralizing charge over all DNA atoms (uniform neutralization).

The system was energy minimized, and dynamics were initiated with the Maxwell distribution of generalized momenta at low temperature. The system was next slowly heated to 293 K and equilibrated for 1 ns. The temperature was maintained by the Berendsen algorithm[40] with a relaxation time of 10 ps. No restraining potential was applied to prevent water evaporation. Instead, water−solute distance was checked every 150 ps and distant water molecules were repositioned randomly in the close proximity of the hydration shell with zero velocities. On average, the number of such molecules was less than one and their effect was considered insignificant. The standard duration of production runs was 10 ns with the coordinates saved every 1 ps. Very similar results were obtained in trial runs of 1 ns with coordinates saved every 100 fs.

The clustering of water molecules was studied as a function of the hydration number (Γ) that varied from 12 to 30 in the case of B-DNA and from 10 to 20 in the case of A-DNA. The water clustering was also studied separately in the major and minor grooves of the double helix. To this end, the sugar−phosphate backbone O2P atoms that face one another in the minor groove of B-DNA were joined by straight lines and the set of the corresponding middle points was used for separating the minor groove water from the rest. All water molecules with oxygens within 7 Å of these reference points were considered as belonging to the minor groove, and the rest of the solvent was attributed to the major groove. Similarly, in the case of the canonical A-DNA, the middle points between sugar−phosphate backbone O1P atoms that face one another in the major groove were used and all water molecules with oxygens within 7 Å of them were considered as belonging to the major groove, while the rest were attributed to the minor groove. In both cases, the middle points form a broken space line separated by about 7 Å from phosphate oxygens and from the bottom of the corresponding groove. Due to fixed regular structures of the canonical A- and B-forms, these procedures provide a clean separation of the two qualitatively different parts of the A- and B-DNA hydration shells.

Water molecules belong to the same cluster if they are connected by a continuous path of hydrogen bonds (H-bonds).[12,41,42] Two water molecules are considered as being H-bonded when the distance between the oxygen atoms is <3.5 Å and the water−water interaction energy is ≤ -2.3 kcal/mol. To locate the percolation threshold of water and to characterize the formation of a spanning water network, various properties of water clusters were calculated for each saved configuration and averaged over 10^4 configurations. First, we have calculated the cluster size distribution (n_S), which is the occurrence probability of clusters of size S measured as the number of water molecules in the cluster. The mean cluster size (S_{mean}) was calculated as

$$S_{mean} = \frac{\sum n_S S^2}{\sum n_S S} \quad (1)$$

excluding the largest cluster from the sum. The probability distribution [$P(S_{max})$] of the size (S_{max}) of the largest water cluster was used for estimating the spanning probability (R), that is, the probability to observe a spanning cluster in an arbitrary chosen configuration. Its value was obtained as an integral of $P(S_{max})$ over $S_{max} > 0.5N_w$, where $N_w = 24\Gamma$ is the total number of water molecules.[15,16,18] Additionally, we have analyzed the fraction S^{av}_{max}/N_w of water molecules in the largest cluster (S^{av}_{max} is the average of S_{max} at a given hydration level).

This parameter is somewhat similar to the percolation probability defined as the fraction of molecules in the spanning cluster.[43]

The ability of the largest water clusters to cover the DNA molecule homogeneously was characterized by the probability distributions of three parameters, namely, the distance (H) between the centers of mass of the largest water cluster and DNA molecule, the radius of gyration (R_g) of the largest cluster, and its maximal extension (L_m), that is, the maximal distance between two water oxygens in the largest cluster. The width of the probability distributions $P(S_{max})$, $P(H)$, $P(R_g)$, and $P(L_m)$ was computed as $\Delta A = \sqrt{\langle (A-A^{av})^2 \rangle / N_w}$, where A stands for any of the four parameters S_{max}, H, R_g, or L_m. The fractal structure of the largest water cluster was evaluated from its radial mass distribution [$m(r)$] defined as the average number of water molecules of the largest cluster found within a cutoff sphere of radius r centered at any member of the largest cluster. This radial mass distribution was fitted to the equation

$$m(r) = a_f r^{d_f} \qquad (2)$$

where d_f and a_f are referred to as the estimated fractal dimension and amplitude, respectively.

3. Results

3.1. General Percolation Properties of DNA Hydration Shells. Earlier studies showed that, in percolation transitions on real biomolecular surfaces, the cluster properties of hydration water generally follow predictions of the percolation theory and that deviations from these laws due to inhomogeneity of biosurfaces are noticeable only below the percolation threshold.[12,16−19,31] The probability distribution [$P(S_{max})$] of the size (S_{max}) of the largest water cluster is one of the properties most sensitive to the percolation transition. Such distributions obtained at various hydration levels for the surfaces of B- and A-DNA molecules are shown in Figure 1. Only the left peak corresponding to nonspanning clusters is seen at low hydrations below the percolation threshold. Accordingly, only the right peak corresponding to the spanning clusters is seen at high hydrations above the percolation threshold. At intermediate hydrations, S_{max} shows a wide probability distribution, with the two peaks almost merged. The most symmetric distribution $P(S_{max})$ is observed at a hydration level where spanning and nonspanning clusters are equally populated, and this hydration corresponds to the midpoint of the percolation transition ($R = 50\%$). The spanning probability [$R(\Gamma)$] estimated from these distributions for A- and B-DNA surfaces (see Methods) is shown in Figure 2 (upper panel). Together with Figure 1, it suggests that the midpoints of the percolation transitions, that are the positions of the inflection points of $R(\Gamma)$ being fitted to sigmoid functions, are close to $\Gamma \approx 14.3$ and 12.9 in B- and A-DNA, respectively. Accordingly, the fraction S^{av}_{max}/N_w of water molecules in the largest cluster, shown in the lower panel of Figure 2, drastically increases when Γ grows from about 13 to 18, indicating the midpoint of the percolation transition in A-DNA at a slightly lower hydration than that in B-DNA.

The evolution of the mean cluster size (S_{mean}) (see Methods) is shown in Figure 3. In a finite system, $S_{mean}(\Gamma)$ should reach a maximum just below the true percolation threshold, and this point is analogous to the maximum of density fluctuations in thermal phase transitions.[43] According to Figure 3, therefore, the true percolation threshold is expected at $\Gamma \gtrsim 14$ for both B- and A-DNA molecules. For both DNA forms, the plots are similar, pointing to the closeness of their percolation thresholds. This similarity is also supported by the variation of the distribution width (ΔS_{max}) shown in the lower panel of Figure 3. The maximal values of ΔS_{max} and, consequently, the strongest variations of the size of the largest cluster occur at $\Gamma \approx 14-15$. Both the fluctuations of the largest cluster size and the density fluctuations in the whole system reach maxima close to the midpoint of the percolation transition, when $R = 50\%$.

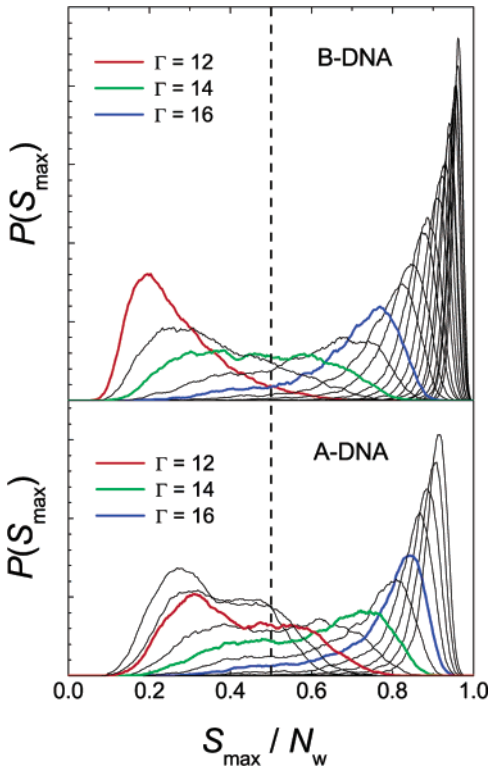

Figure 1. Probability distribution [$P(S_{max})$] of the size (S_{max}) of the largest water cluster on B- and A-DNA surfaces with hydration numbers (Γ) from 10 to 30. Selected hydrations are shown by solid colored traces as indicated in the figure.

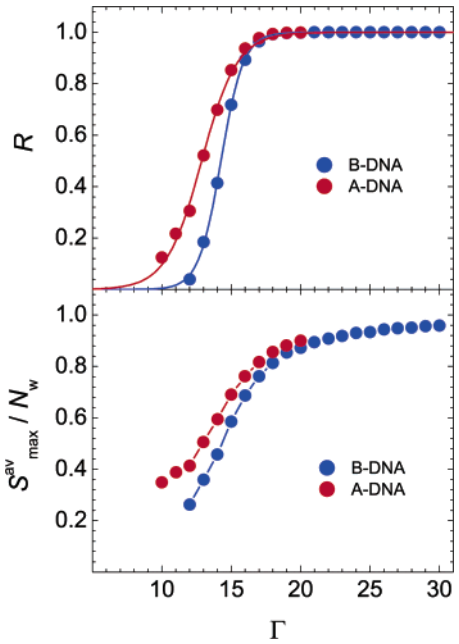

Figure 2. Probability (R) of observing a spanning water cluster (upper panel) and the fraction S^{av}_{max}/N_w of water molecules in the largest cluster (lower panel) as functions of hydration number (Γ) for B- and A-DNA surfaces. Sigmoid fits are shown by solid lines in the upper panel.

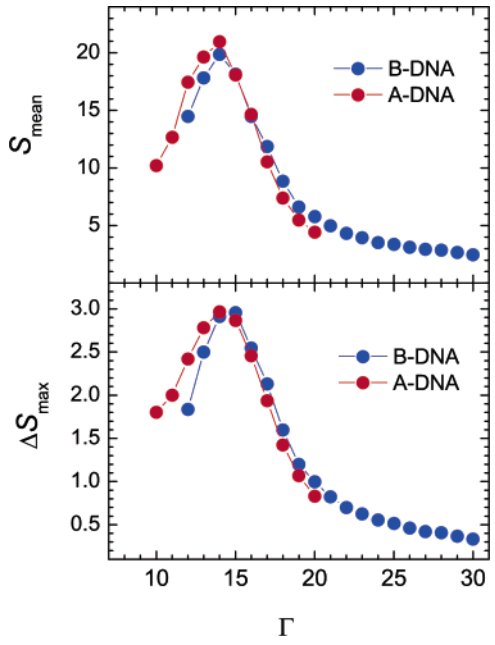

Figure 3. Mean cluster size (S_{mean}) (upper panel) and the width (ΔS_{max}) of the probability distribution [$P(S_{max})$] of the size of the largest water cluster (lower panel) as functions of hydration number (Γ).

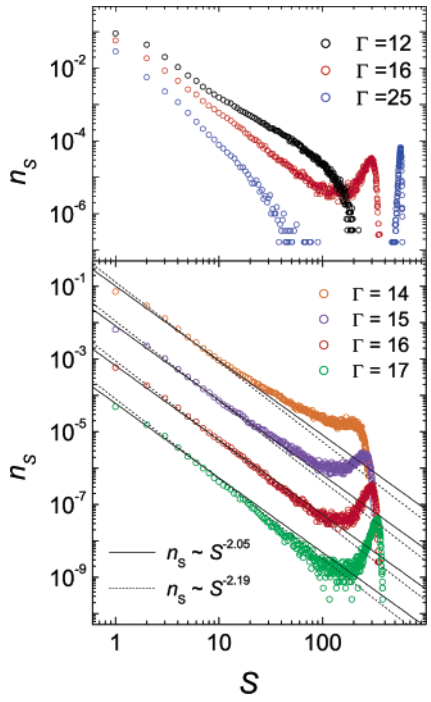

Figure 4. Distribution (n_S) of the size of water clusters at the surface of B-DNA for representative hydration numbers (Γ). The universal power laws expected for 2D and 3D percolation transitions are shown by solid and dotted lines, respectively.

The true percolation threshold can be located by using the cluster size distribution (n_S) that, at the true percolation threshold, should obey a universal power law, $n_S \sim S^{-\tau}$, in the widest range of cluster size (S). The exponent τ depends on the spatial dimension of the system considered and equals approximately 2.05 and 2.19 for 2D and 3D systems, respectively.[43] The n_S distribution strongly changes with hydration, and strong deviations from the power law behavior are seen at both the lowest and highest hydration levels (Figure 4, upper panel). However, in the vicinity of the percolation transition, the power law behavior is indeed observed in the widest range

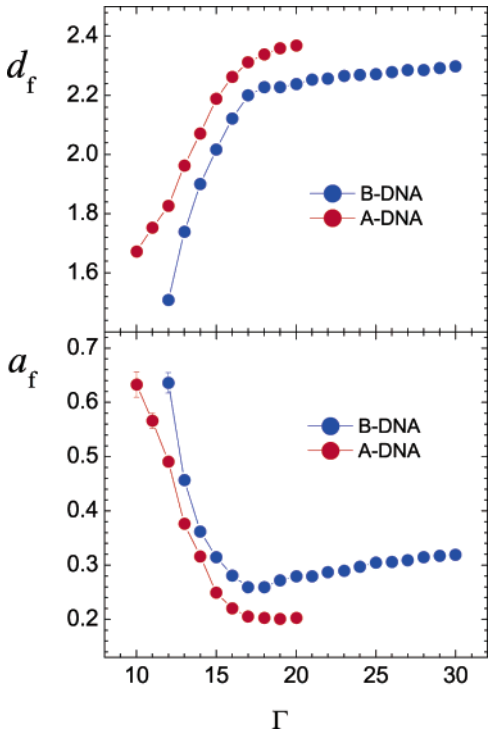

Figure 5. Fractal dimension (d_f) and amplitude (a_f) (see eq 2) of the largest water cluster at the surface of B- and A-DNA under various hydrations.

of the cluster sizes (S) (Figure 4, lower panel). Evidently, the range of validity of the power law for n_S is the largest with Γ ≈ 15 and 16. This conclusion does not depend on the assumed dimensionality of the system being studied, that is, water adsorbed at the DNA surface. Due to the grooved shape of the DNA double helix, the 2D character of its hydration water is not obvious. That is why, in Figure 4, the reference power laws are shown for both the 2D and 3D cases. For A-DNA, the evolution of n_S distributions with hydration turned out to be very similar to that in Figure 4, with the estimated percolation threshold almost identical to that of B-DNA. In both of these cases, the true percolation threshold is attributed to a hydration number of $\Gamma = 15.5 \pm 0.5$, that is, higher than the midpoints of the percolation transitions in B-DNA (Γ ≈ 14.3) and A-DNA (Γ ≈ 12.9). The spanning probability (R) at the percolation threshold is about 90%, which is close to the values observed at the true percolation transition of water at the surface of a lysozyme molecule (about 90%) and at the surfaces of smooth spheres (from 70 to 90%, depending on a sphere size).[16]

The dimensionality of the largest water cluster is characterized by the effective fractal dimension (d_f) obtained from its mass distribution (see Methods). Variations of the estimated fractal parameters with hydration are shown in Figure 5. In ideal 2D and 3D systems, the percolation threshold is characterized by $d_f \approx 1.89$ and 2.53, respectively.[43] Figure 5 indicates that hydration water at the B-DNA surface represents a quasi-2D system. Deviations from a 2D behavior are larger for A-DNA, indicating a more heterogeneous distribution of hydration water. At Γ ≈ 17, both $d_f(\Gamma)$ and $a_f(\Gamma)$ dependences display qualitative changes. The slopes of the $d_f(\Gamma)$ plots drastically fall for both A- and B-DNA (Figure 5, upper panel). Simultaneously, the amplitude (a_f) seems to reach a lower limit and even shows a shallow minimum in the case of B-DNA (Figure 5, lower panel). This behavior is not sensitive to the fitting procedure, notably, to the interval of r used for the fits. Apparently, a qualitative

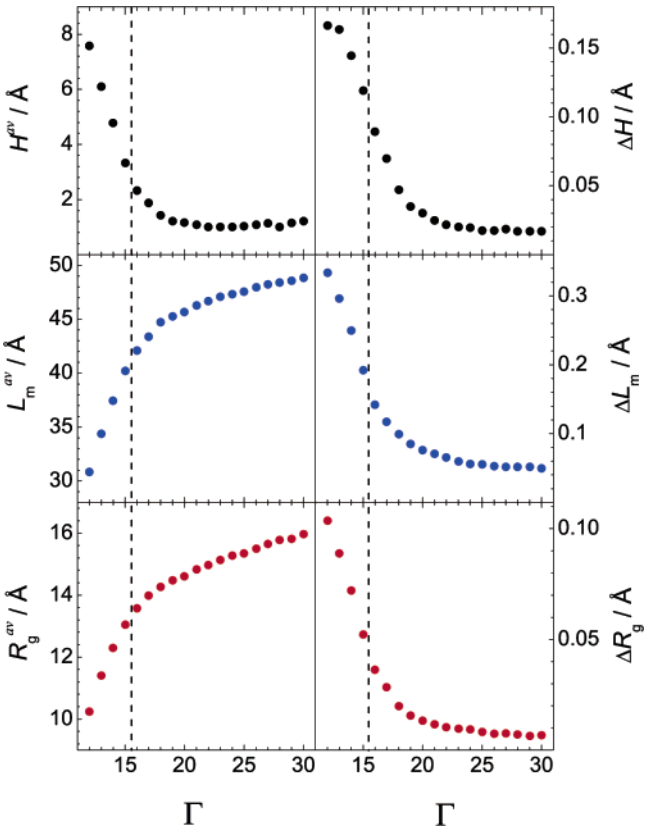

Figure 6. Left panels: the average separation of the center of mass of the largest water cluster from that of DNA (H), the maximum linear extension (L_m), and the radius of gyration (R_g) of the largest water cluster at the surface of B-DNA. Right panels: the widths of the corresponding probability distributions. The hydration number corresponding to the true percolation threshold is marked by the vertical dashed lines.

change of the internal structure of the largest water cluster takes place just above the percolation threshold.

The spanning character of the largest water cluster may be characterized by the distance (H) between the centers of mass of the largest water cluster and the DNA molecule as well as the radius of gyration (R_g) and the maximal extension (L_m) of the largest water cluster. The probability distributions of H, R_g, and L_m show a two-peak structure in the wide range of hydrations below the percolation threshold, but above this threshold, a single narrow peak appears (see, for instance, the distributions for H in Figure 4 of ref 31). Similar behavior was earlier observed for hydration water at model hydrophilic surfaces and protein surfaces.[17,18] In the left panel of Figure 6, the average values of H, R_g, and L_m at the surface of B-DNA are shown as functions of hydration number. Under low hydration, the center of mass of the largest water cluster on average is far from that of DNA, which means that such clusters do not envelope the hydrated molecule. The value of H drastically decreases when the system approaches the water percolation threshold (vertical line in Figure 6) and practically equals zero above it, indicating a homogeneous coverage of DNA by the H-bonded network of hydration water. The radius of gyration (R_g) and the maximal extension (L_m) of the largest water cluster behave similarly. Below the percolation threshold, they increase strongly with Γ, whereas, above the percolation threshold, this growth becomes approximately linear and relatively slow. Besides, the widths of all probability distributions (see Methods) dramatically fall when Γ passes the percolation threshold (see the right panel of Figure 6).

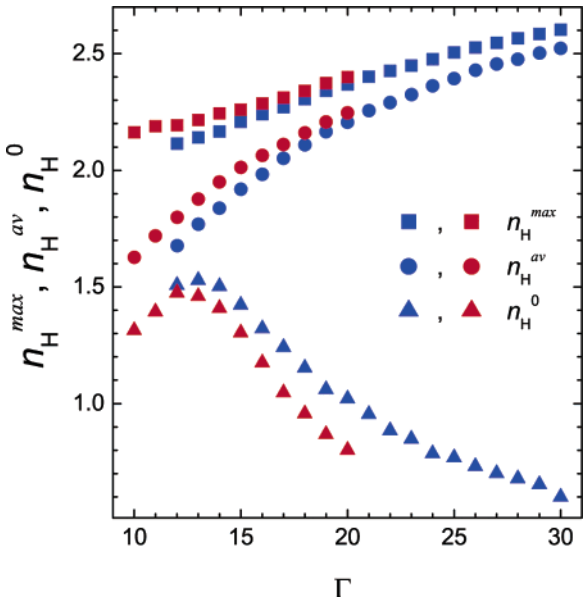

Figure 7. Average number of H-bonded neighbors as a function of hydration number (Γ) for all water molecules (n_H^{av}), for water molecules of the largest cluster only (n_H^{max}), and for water molecules that do not belong to the largest cluster (n_H^0). Data for B- and A-DNA are shown by blue and red symbols, respectively.

The water−water H-bonding is conventionally characterized by the average number of H-bonded neighbors (n_H^{av}) which gradually grows with Γ (Figure 7). A similar parameter calculated for the largest cluster (n_H^{max}) shows a much slower increase, indicating that the growth of the largest cluster occurs via attachment of smaller clusters, which does not change the internal structure of the largest cluster.[44] The average number (n_H^0) of H-bonded neighbors averaged over all clusters except the largest one passes through a maximum at $\Gamma \approx 13$, that is, just below $\Gamma \approx 14$ where the maximum of the mean cluster size (S_{mean}) is observed (see Figure 3).

3.2. Specific Clustering of Water in DNA Grooves. The surface of the double helical DNA is usually considered as involving at least two distinct nonoverlapping parts with qualitatively different properties, namely, the major and minor grooves. In B-DNA, the minor groove is narrow and deep, whereas the major groove is very wide and its surface is easily accessible from solution. In contrast, in the A-form of DNA, the minor groove represents almost a flat exposed surface, while the major groove becomes very deep and narrow. In A-DNA, the opening of the major groove is probably blocked by free metal ions sandwiched between the two opposed phosphate arrays.[27,45] During the B-to-A transition, the major DNA groove collapses around these ions, while the minor groove turns inside out, completely losing its initial properties. All of these events are certainly related to changes in the water structure. To get insight into their mechanisms, hydration and water clustering in the two DNA grooves should be studied separately. To this end, in each saved configuration, the hydration shells of A- and B-DNA were divided into two parts. The main idea was to find the closed compartments where hydration conditions do not change with Γ. It was anticipated that the minor groove of B-DNA and the major groove of A-DNA probably represent the natural such compartments, and the procedure used for water partitioning was adjusted accordingly (see Methods). In the following discussion, the B-DNA major groove water involves all water except that enclosed in the minor groove, and, vice versa, the minor groove water of A-DNA involves all water except that enclosed in the major groove.

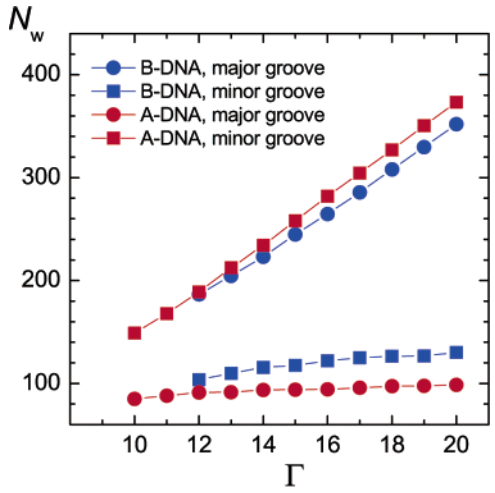

Figure 8. Number of water molecules in the major and minor grooves of B- and A-DNA as functions of hydration number (Γ).

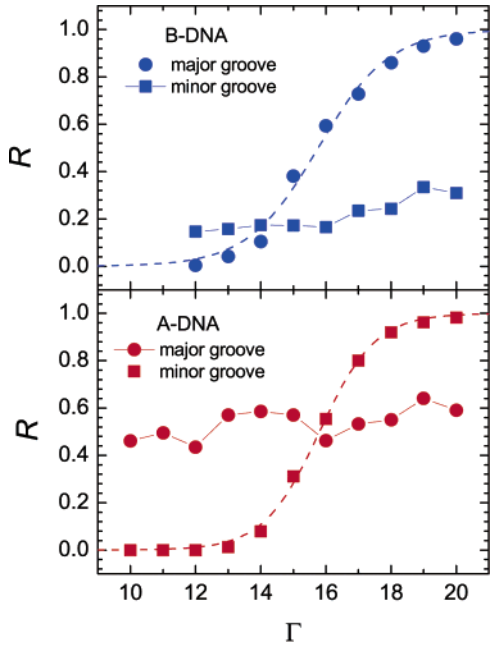

Figure 9. Probability (R) of observing a spanning water cluster in the major and minor grooves of B- and A-DNA molecules as functions of hydration number (Γ).

Figure 8 shows variation of the number of water molecules in the grooves of B- and A-DNA with Γ. As expected, the weight of the hydration shells in the minor groove of B-DNA, and the major groove of A-DNA, remains very stable. Even with Γ reduced below the percolation threshold, the number of water molecules in these compartments changes insignificantly. Variations of Γ mainly affect the remaining part of water. The clustering behavior is also radically different. The probability (R) to observe a spanning water cluster in the major groove of B-DNA and the minor groove of A-DNA exhibits a sigmoid behavior typical for percolation transitions, with inflection points ($R \approx 50\%$) at $\Gamma \approx 15.8$ in both cases (Figure 9). The spanning probabilities (R) of the largest water cluster in the minor groove of B-DNA and in the major groove of A-DNA show only a weak positive trend with hydration number. When the percolation transition occurs in the whole hydration shell of DNA, the probability to observe a spanning cluster in the minor groove of B-DNA and the major groove of A-DNA is about 20 and 50%, respectively. It means that, although water in the relatively isolated B-DNA minor and the A-DNA major grooves contribute

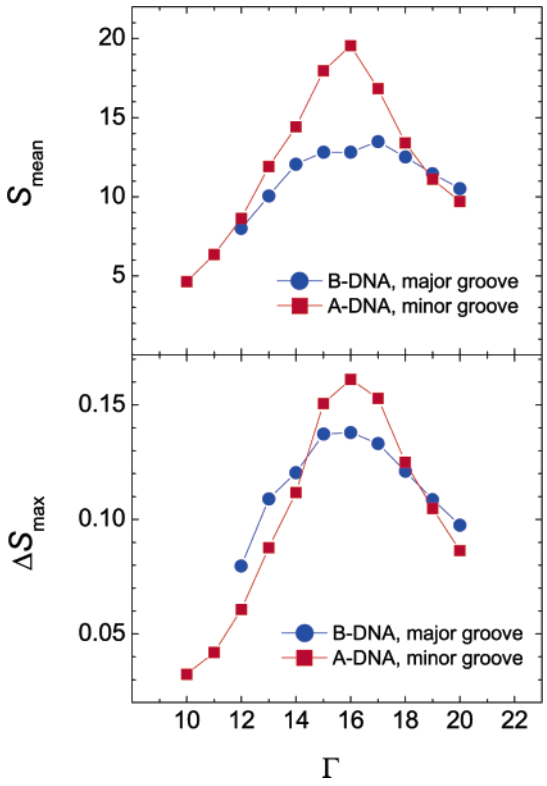

Figure 10. Mean size (S_{mean}) of water clusters on B- and A-DNA surfaces (upper panel) and the width (ΔS_{max}) of the probability distribution of the size (S_{max}) of the largest water cluster (lower panel) as functions of hydration number (Γ).

to the largest water cluster in the whole hydration shell, the spanning water cluster appears permanently due to the percolation transition in the opposite exposed grooves. This complex picture is supported by the behavior of the mean cluster size (S_{mean}) and the width (ΔS_{max}) of the probability distribution of the largest water cluster shown in Figure 10. The same parameters calculated for the exposed grooves of the two DNA forms show maxima in the hydration range where the spanning probability is about 50%.

3.3. Free Ions and Water Percolation Transition. The key role of free metal ions in low hydration polymorphism of DNA was well established by earlier experimental studies.[46] By changing the amount and type of ions, one can shift the midpoints of polymorphic transitions and even their pathways.[47] Almost nothing is known about the detailed mechanisms involved in such effects, and theoretical models are also usually absent. As a step toward elucidation of these problems, here we studied how free sodium ions available in our simulations affect water clustering and the percolation transition. Earlier reports suggested that, without free ions, small hydration shells around charged DNA fragments are inherently unstable.[36] Therefore, to run similar calculations without ions, we decided to neutralize DNA artificially. Neutralization of DNA has been used in simulations since long ago,[48] and usually, this is done by reducing phosphate charges. Some results obtained in simulations with electrostatically neutral B-DNA obtained by reducing charges of OP atoms are shown in Figures 11−13. It turns out that water in this system does not show a percolation transition in the course of gradual hydration. The probability distribution [$P(S_{max})$] of the size of the largest cluster behaves as if the system consists of small water droplets that merge into one large water patch with increased hydration (Figure 11, upper panel). This scenario is also suggested by the absence of the sigmoidal behavior for spanning probability (R), the absence

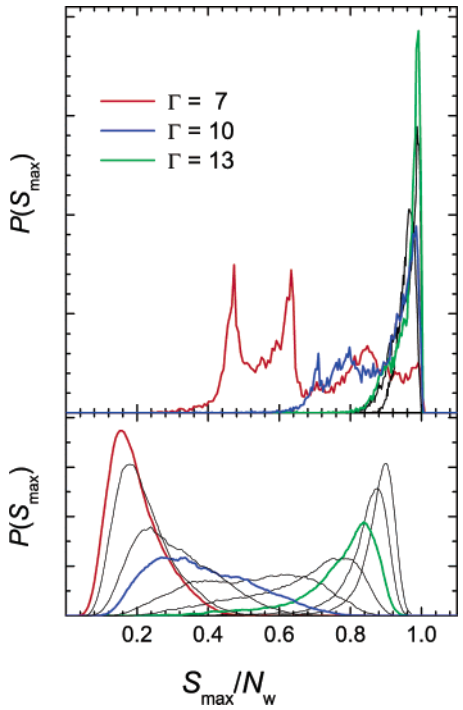

Figure 11. Probability distributions of the size (S_{max}) of the largest water cluster at artificially neutralized B-DNA surfaces at various hydration numbers (Γ) from 10 to 30, with phosphate neutralization (upper panel) and uniform neutralization (lower panel). Selected hydration levels are shown by the solid colored traces as indicated in the figure.

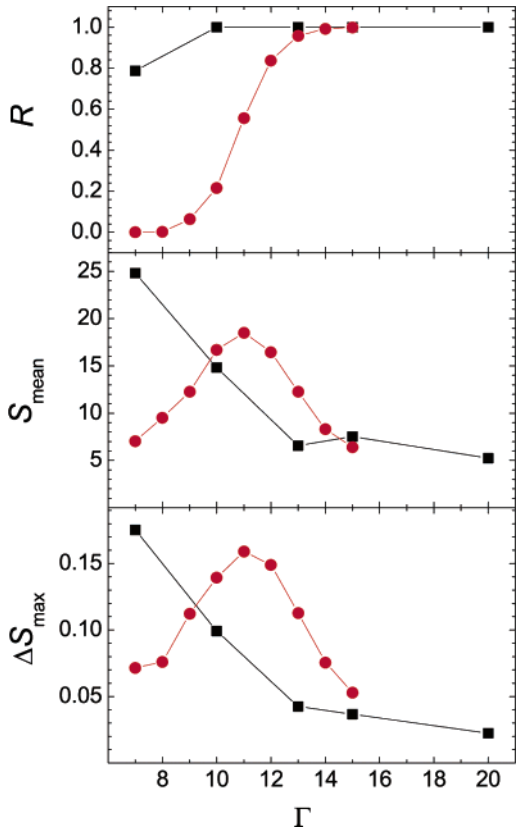

Figure 12. Probability (R) of observing a spanning water cluster (upper panel), the mean cluster size (S_{mean}) (middle panel), and the width (ΔS_{max}) of the probability distribution of the size of the largest cluster (lower panel), as functions of hydration number (Γ) for uniform neutralization (red circles) and phosphate neutralization (black squares) of the B-DNA surface.

of a maximum of S_{mean}, and a monotonous change of ΔS_{max} (Figure 12). Formation of a large continuous water patch is also evident from the cluster size distribution shown in Figure 13. Such behavior of n_S is typical for water near hydrophobic surfaces or in mixtures with hydrophobic solutes,[49] which is surprising because, even with phosphates neutralized, the DNA surface remains highly polar.

The foregoing results suggested that free sodium ions play a crucial role in construction of water networks on the DNA surface or modify the electrostatic field in its environment so that hydration water can better adhere. It turned out, however, that the behavior of hydration water near neutral DNA depends upon how its surface was neutralized. Two alternative possibilities were checked. In the first case, we distributed the neutralizing charge over the whole system including DNA and water. In the second case, the neutralizing charge was uniformly distributed between all DNA atoms. The hydration water behaved similarly in both of these cases, and Figures 11−13 demonstrate some of the results obtained with the second option. It is seen that water undergoes a normal percolation transition with increasing Γ. The probabilities $P(S_{max})$, shown in the lower panel of Figure 11 for various Γ, indicate that the spanning water cluster exists with a probability (R) about 50% somewhere between Γ = 10 and 11, which agrees with the sigmoidal behavior of R shown in Figure 12. The maxima of S_{mean} and ΔS_{max} indicate the true percolation transition of water at Γ > 11. The cluster size distribution (n_S) shown in Figure 13 locates the threshold hydration at about Γ = 12.5 ± 0.5, that is, three units lower than in the presence of free ions.

The qualitative difference between the above two electrostatically neutral DNA models is revealed in Figure 14. With reduced charges of OP atoms (left panel), the sugar−phosphate backbone behaves as a hydrophobic boundary. The hydration shell is divided into two separate compartments corresponding to the

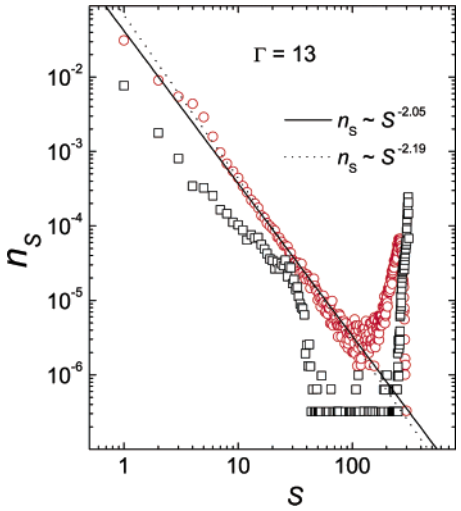

Figure 13. Cluster size distribution (n_S) of water clusters for uniform neutralization (red circles) and phosphate neutralization (black squares) of the B-DNA surface at Γ = 13. The universal power laws expected at 2D and 3D percolation transitions are shown by solid and dotted lines, respectively.

minor and major grooves, and water is confined in reduced zones where it accumulates in continuous patches. In contrast, with uniform neutralization (right panel), water tends to cover the sugar−phosphate backbone by a thin spanning H-bonded network. Note that the number of water molecules is exactly identical in these two systems. The radically different hydration pattern in the left panel of Figure 14 probably results from the geometry and a specific charge distribution in the sugar−

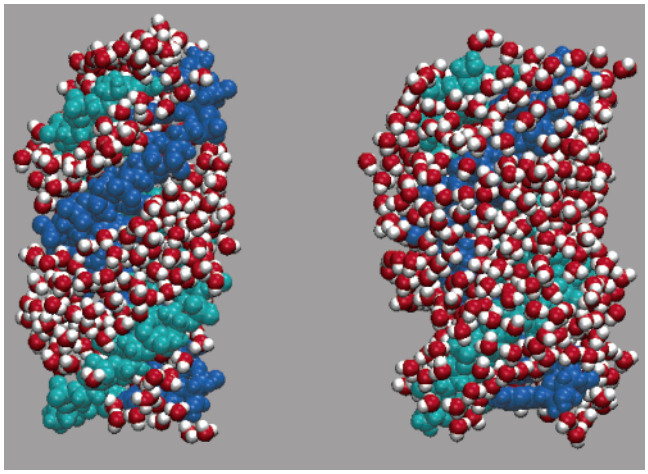

Figure 14. Representative snapshots of hydration shells at an artificially neutralized B-DNA surface: left panel, phosphate neutralization; right panel, uniform neutralization. The hydration number is $\Gamma = 13$ in both cases. The two complementary DNA strands are colored by cyan and blue, respectively.

phosphate backbone because it remains very polar and does not resemble typical hydrophobic substances.

4. Discussion

The results presented here evidence that the spanning H-bonded network of hydration water, that homogeneously covers the DNA molecule under high relative humidity, first appears via a quasi-2D percolation transition upon gradually increasing hydration. With a neutralizing amount of sodium ions in the hydration shell, the percolation threshold is almost identical for B- and A-DNA forms and is close to $\Gamma = 15.5 \pm 0.5$. At the threshold hydration, the minor groove of B-DNA is already filled with water, and the quasi-2D percolation transition results in the formation of a spanning water network in the major groove. In contrast, in A-DNA, the major groove is completely filled well below the percolation threshold, and the transition leads to the formation of a spanning water network in the minor groove. In view of this qualitative difference, the closeness of the percolation thresholds in the two systems seems perplexing. At this time, we cannot say if there are some physical reasons behind this finding or if it is a simple coincidence.

It was shown earlier that the percolation threshold of hydration water is rather universal when it is described using the average number (n_H^{av}) of water−water H-bonds.[50] Here, we have found that the spanning network at the DNA surface occurs when $n_H^{av} \approx 2.0$ at ambient temperature. This value is slightly lower than $n_H^{av} = 2.3$ characteristic of the percolation transitions at the surface of a single lysozyme molecule and coincides with n_H obtained for lysozyme powder. Apparently, in the latter case as well as for the DNA surface, the structure of the ramified spanning water network exhibits a trend to three-dimensionality, which results in the decrease of n_H^{av} at the percolation threshold.[42,44,50]

The threshold hydration of $\Gamma = 15.5 \pm 0.5$ is surprisingly close to the experimental midpoint of the transition between A- and B-forms of DNA, suggesting that its mechanism and the driving forces are somehow connected with water percolation. A simplistic view would suggest that the percolation transition occurs around either A- or B-form and pushes the DNA structure into the alternative form. However, the true scenario is probably more complex. The experimental A ↔ B transition midpoint at $\Gamma \approx 15$ corresponds to a generic or random sequence DNA, but for special sequences, it is found somewhat above and below the average.[51,52] At the same time, our preliminary studies indicate that the water percolation transition on the B-DNA surface is not sequence dependent (unpublished results of the authors). Therefore, the poly(dG)·poly(dC) duplex, that takes the A-form under higher relative humidity, should do that above the percolation threshold, whereas sequences rich in poly(dA)·poly(dT) tracts, that go to the A-form at lower hydration, perhaps stay in the B-form until the percolation transition.

The results reported here as well as earlier experimental and computational observations agree with the following mechanism of A ↔ B transitions.[27,28,31,45] When B-DNA hydration is reduced, and the H-bonded water network approaches the percolation threshold, free sodium ions lose translational entropy and tend to accumulate in the major groove. This increases the electrostatic tension across the major groove and eventually leads to intraduplex electrostatic condensation that pushes DNA from the B- to A-form. Depending upon the DNA sequence, this occurs farther or closer to the percolation threshold but always somewhat above it. This implies that, of the two transitions considered here, this is water percolation around the A-form that should be considered as the most common case. In contrast, if a particular sequence stays in the B-form until the percolation transition, it probably does not go to the A-form at all, as, for instance, the fiber poly(dA)·poly(dT) DNA.[21] Below the percolation threshold, sodium ions are frozen at fixed positions near DNA and the forces that push it toward the A-form can no longer grow. The closeness of the water percolation threshold to the experimental midpoint of A ↔ B transitions suggests that random sequence DNA strongly prefers the B-form and transitions to the A-form start only when the spanning H-bonded water network approaches its limit.

Considering possible intrinsic properties of spanning H-bonded water networks that can play a casual role in the above scenario, two effects should be distinguished. The first is the long-range H-bonded connectivity that drastically increases at the percolation threshold, specifically affecting the ion mobility.[31] The second factor manifests itself as the maximum of the mean cluster size and the distribution width of the size of the largest water cluster at $\Gamma \approx 14$ (Figure 3). As the mean cluster size in the percolation transition is an analogue of the susceptibility in the thermal phase transition,[43] the largest density fluctuations of water may be expected at this hydration level. The water density fluctuations strongly increased at the midpoint of the percolation transition should additionally destabilize DNA. Both of these factors may be involved in the detailed mechanisms of the low hydration polymorphic transitions in DNA. The B ↔ A transition in aqueous solutions of nonpolar alcohols[29] can occur by a similar mechanism.[27] It is known that the increase of solute concentration in water ultimately causes a breakdown of the percolating water network via a percolation transition.[42,53] One may expect that the break of the spanning network of hydration water due to addition of alcohols is mechanistically similar to its break upon dehydration.

We were strongly surprised to find that artificial neutralization of phosphate charges on DNA abolishes the percolation property of its hydration shell. On the face of it, complete or partial neutralization of phosphates looks to be a very reasonable approximation, and it was often used in the earlier literature since the very first pioneering studies.[48] It turns out that this apparently reasonable modification makes the DNA surface strongly heterogeneous so that hydration water can no longer form ramified networks on it. In contrast, if the compensating

charge is distributed homogeneously between all atoms, the DNA surface retains its original properties and hydration water undergoes a quasi-2D percolation transition. In this case, the percolation threshold is found at a hydration of $\Gamma = 12.5 \pm 0.5$, that is about three water molecules less than in the case of DNA with Na^+ ions. These additional water molecules are probably engaged in ion hydration, which reduces their ability to participate in spanning H-bonded water networks.

A number of aspects of ion involvement in DNA hydration remain controversial and require additional studies. For instance, in bulk aqueous solutions, trivalent cations $[Co(NH_3)_6]^{3+}$ can reportedly induce a B-to-A transition in DNA via major groove binding, that is, by using essentially the same mechanism as that described above.[54] It is known that Mg^{2+} ions bind to DNA similarly to $[Co(NH_3)_6]^{3+}$.[55] Surprisingly, Mg^{2+} ions do not promote B-to-A transition; moreover, high concentrations of $MgCl_2$ stabilize the B-form and shift the midpoint of A $\leftrightarrow$ B transitions toward lower relative humidities.[54,56] Here, we found that the simple presence of ions near a hydrophilic surface can significantly shift the water percolation threshold. One may expect that the magnitude and the sign of this effect depends upon ion types and charges, as well as the properties of negative co-ions. Our computational observations suggest that ion effects on the state of DNA may be very complex because in addition to direct electrostatic interactions they can act indirectly by changing the properties of the spanning H-bonded water networks around DNA.

Acknowledgment. I.B., A.K., and A.O. acknowledge financial support from DFG Forschergruppe 436.

References and Notes

(1) Gascoyne, P. R.; Pethig, R.; Szent-Gyorgyi, A. *Proc. Natl. Acad. Sci. U.S.A.* **1981**, *78*, 261−265.
(2) Careri, G.; Giansanti, A.; Rupley, J. A. *Proc. Natl. Acad. Sci. U.S.A.* **1986**, *83*, 6810−6814.
(3) Careri, G.; Giansanti, A.; Rupley, J. A. *Phys. Rev. A* **1988**, *37*, 2703−2705.
(4) Rupley, J. A.; Siemankowski, L.; Careri, G.; Bruni, F. *Proc. Natl. Acad. Sci. U.S.A.* **1988**, *85*, 9022−9025.
(5) Bruni, F.; Careri, G.; Leopold, A. C. *Phys. Rev. A* **1989**, *40*, 2803−2805.
(6) Bruni, F.; Careri, G.; Clegg, J. S. *Biophys. J.* **1989**, *55*, 331−338.
(7) Rupley, J. A.; Careri, G. *Adv. Protein Chem.* **1991**, *41*, 37−172.
(8) Klammler, F.; Kimmich, R. *Croat. Chem. Acta* **1992**, *65*, 455−470.
(9) Konsta, A. A.; Laudat, J.; Pissis, P. *Solid State Ionics* **1997**, *97*, 97−104.
(10) Haranczyk, H. *On water in extremely dry biological systems*; Jagiellonian University Press: Krakow, Poland, 2003.
(11) Sokolowska, D.; Krol-Otwinowska, A.; Moscicki, J. K. *Phys. Rev. E* **2004**, *70*, 052901.
(12) Oleinikova, A.; Smolin, N.; Brovchenko, I.; Geiger, A.; Winter, R. *J. Phys. Chem. B* **2005**, *109*, 1988−1998.
(13) Kuntz, I. D.; Kauzmann, W. *Adv. Protein Chem.* **1974**, *28*, 239−345.
(14) Brovchenko, I.; Oleinikova, A. In *Handbook of Theoretical and Computational Nanotechnology*; Rieth, M., Schommers, W., Eds.; American Scientific Publishers: Stevenson Ranch, CA, 2006; Vol. 9, Chapter 3, pp 109−206.
(15) Oleinikova, A.; Brovchenko, I.; Geiger, A. *Physica A* **2006**, *364*, 1−12.
(16) Oleinikova, A.; Brovchenko, I. *Mol. Phys.* **2006**, *104*, 3841−3855.
(17) Smolin, N.; Oleinikova, A.; Brovchenko, I.; Geiger, A.; Winter, R. *J. Phys. Chem. B* **2005**, *109*, 10995−11005.
(18) Brovchenko, I.; Krukau, A.; Smolin, N.; Oleinikova, A.; Geiger, A.; Winter, R. *J. Chem. Phys.* **2005**, *123*, 224905.
(19) Oleinikova, A.; Smolin, N.; Brovchenko, I. *J. Phys. Chem. B* **2006**, *110*, 19619−19624.
(20) Saenger, W. *Principles of Nucleic Acid Structure*; Springer-Verlag: New York, 1984.
(21) Leslie, A. G. W.; Arnott, S.; Chandrasekaran, R.; Ratliff, R. L. *J. Mol. Biol.* **1980**, *143*, 49−72.
(22) Saenger, W.; Hunter, W. N.; Kennard, O. *Nature* **1986**, *324*, 385−388.
(23) Texter, J. *Prog. Biophys. Mol. Biol.* **1979**, *33*, 83−97.
(24) van Dam, L.; Korolev, N.; Nordenskild, L. *Nucleic Acids Res.* **2002**, *30*, 419−428.
(25) van Dam, L.; Levitt, M. H. *J. Mol. Biol.* **2000**, *304*, 541−561.
(26) Fuller, W.; Forsyth, T.; Mahendrasingam, A. *Philos. Trans. R. Soc. London, Ser. B* **2004**, *359*, 1237−48.
(27) Mazur, A. K. *J. Am. Chem. Soc.* **2003**, *125* (26), 7849−7859.
(28) Mazur, A. K. *J. Chem. Theory Comput.* **2005**, *1*, 325−336.
(29) Ivanov, V. I.; Minchenkova, L. E.; Minyat, E. E.; Schyolkina, A. K. *Cold Spring Harbor Symp. Quant. Biol.* **1983**, *47*, 243−250.
(30) Malenkov, G.; Minchenkova, L.; Minyat, E.; Schyolkina, A.; Ivanov, V. *FEBS Lett.* **1975**, *51*, 38−42.
(31) Brovchenko, I.; Krukau, A.; Oleinikova, A.; Mazur, A. K. *Phys. Rev. Lett.* **2006**, *97* (13), 137801(4).
(32) Warman, J. M.; de Haas, M. P.; Rupprecht, A. *Chem. Phys. Lett.* **1996**, *249*, 319−322.
(33) Arnott, S.; Hukins, D. W. L. *Biochem. Biophys. Res. Commun.* **1972**, *47*, 1504−1509.
(34) Cornell, W. D.; Cieplak, P.; Bayly, C. I.; Gould, I. R.; Merz, K. M.; Ferguson, D. M.; Spellmeyer, D. C.; Fox, T.; Caldwell, J. W.; Kollman, P. A. *J. Am. Chem. Soc.* **1995**, *117* (19), 5179−5197.
(35) Jorgensen, W. L.; Chandreskhar, J.; Madura, J. D.; Impey, R. W.; Klein, M. L. *J. Chem. Phys.* **1983**, *79*, 926−935.
(36) Mazur, A. K. *J. Am. Chem. Soc.* **2002**, *124* (49), 14707−14715.
(37) Mazur, A. K. *J. Am. Chem. Soc.* **1998**, *120* (42), 10928−10937.
(38) Mazur, A. K. *J. Chem. Phys.* **1999**, *111* (4), 1407−1414.
(39) Essmann, U.; Perera, L.; Berkowitz, M. L.; Darden, T.; Lee, H.; Pedersen, L. G. *J. Chem. Phys.* **1995**, *103*, 8577−8593.
(40) Berendsen, H. J. C.; Postma, J. P. M.; van Gunsteren, W. F.; DiNola, A.; Haak, J. R. *J. Chem. Phys.* **1984**, *81*, 3684−3690.
(41) Geiger, A.; Stillinger, F.; Rahman, A. *J. Chem. Phys.* **1979**, *70*, 4185−4193.
(42) Oleinikova, A.; Brovchenko, I.; Geiger, A.; Guillot, B. *J. Chem. Phys.* **2002**, *117*, 3296−3304.
(43) Stauffer, D. *Introduction to percolation theory*; Taylor and Francis: London and Philadelphia, PA, 1985.
(44) Pártay, L. P.; Jedlovszky, P.; Oleinikova, A.; Brovchenko, I. *Phys. Chem. Chem. Phys.*, in press.
(45) Cheatham, T. E., III; Crowley, M. F.; Fox, T.; Kollman, P. A. *Proc. Natl. Acad. Sci. U.S.A.* **1997**, *94*, 9626−9630.
(46) Ivanov, V. I.; Minchenkova, L. E.; Minyat, E. E.; Frank-Kametetskii, M. D.; Schyolkina, A. K. *J. Mol. Biol.* **1974**, *87*, 817−833.
(47) Zimmerman, S. B.; Pheiffer, B. H. *J. Mol. Biol.* **1980**, *142*, 315−330.
(48) Zhurkin, V. B.; Lysov, Y. P.; Ivanov, V. I. *Nucleic Acids Res.* **1979**, *6* (3), 1081−1096.
(49) Brovchenko, I.; Geiger, A.; Oleinikova, A. *J. Chem. Phys.* **2004**, *120*, 1958−1972.
(50) Oleinikova, A.; Brovchenko, I.; Smolin, N.; Krukau, A.; Geiger, A.; Winter, R. *Phys. Rev. Lett.* **2005**, *95*, 247802.
(51) Becker, M. M.; Wang, Z. *J. Biol. Chem.* **1989**, *265*, 4163−4167.
(52) Tolstorukov, M. Y.; Ivanov, V. I.; Malenkov, G. G.; Jernigan, R. L.; Zhurkin, V. B. *Biophys. J.* **2001**, *81*, 3409−3421.
(53) Dougan, L.; Bates, S. P.; Hargreaves, R.; Fox, J. P.; Crain, J.; Finney, J. L.; Reat, V.; Soper, A. K. *J. Chem. Phys.* **2004**, *121*, 6456−6462.
(54) Xu, Q.; Shoemaker, R. K.; Braunlin, W. H. *Biophys. J.* **1993**, *65*, 1039−1049.
(55) Robinson, H.; Gao, Y.-G.; Sanishvili, R.; Joachimiak, A.; Wang, A. H.-J. *Nucleic Acids Res.* **2000**, *28*, 1760−1766.
(56) Schultz, J.; Rupprecht, A.; Song, Z.; Piskur, J.; Nordenskiold, L.; Lahajnar, G. *Biophys. J.* **1994**, *66*, 810−819.